



Original Research Article

View Article Online | View Journal

Bifunctional Biochar-Supported Catalysts for Efficient Hydrodeoxygenation of Pyrolytic Oil Derived from Oil Palm Shells

Junifa Layla Sihombing* , Ahmad Nasir Pulungan , Herlinawati Herlinawati, Tiara Ramadhani, Sella Naomi Br Sinaga, Salaisa Salaisa, Dika Fahreza, Muhammad Fatra Arganda Saragih

Department of Chemistry, Faculty of Mathematics and Natural Sciences, Universitas Negeri Medan, Jl. Willem Iskandar Pasar V Medan Estate, Medan 20221, Indonesia

ARTICLE INFORMATION

Submitted: 2025-10-14
 Revised: 2025-12-26
 Accepted: 2026-01-22
 Published: 2026-01-25
 Manuscript ID: [AJGC-2510-1846](#)
 DOI: [10.48309/ajgc.2026.552702.1846](#)

KEYWORDS

Bimetallic catalysts
 Activated biochar
 Hydrodeoxygenation
 Oil palm shells
 Pyrolytic oil

ABSTRACT

This study examines the efficacy of bifunctional biochar-based catalysts in the hydrodeoxygenation (HDO) of pyrolytic bio-oil from oil palm shells. Biochar was produced via pyrolysis and modified with Co-Mo and Ni-Mo to enhance catalytic effectiveness. Characterization revealed that activation increased the biochar's surface area significantly from 10.597 m²/g to 218.964 m²/g, although metal impregnation caused a slight reduction. The HDO process in a fixed-bed reactor showed optimal results at 300 °C, with varying liquid product yields for different catalysts. GC-MS analysis indicated a reduction in oxygenated compounds post-HDO, with specific catalysts achieving notable hydrocarbon formation and selectivity towards phenols. The upgraded bio-oil demonstrated enhanced physicochemical properties, making it more suitable as a biofuel. The study emphasizes the potential of biochar-supported bimetallic catalysts in bio-oil upgrading, highlighting the advantages of Co-Mo/A-Biochar and Ni-Mo/A-Biochar. These results illustrate the viability of palm shell waste in sustainable biofuel production, addressing environmental and energy concerns.

© 2026 by SPC (Sami Publishing Company), Asian Journal of Green Chemistry, Reproduction is permitted for noncommercial purposes.

Graphical Abstract



Introduction

Palm oil is one of the most versatile vegetable oils worldwide, used in cooking oil, margarine, detergents, cosmetics, and increasingly as a biofuel feedstock as countries diversify their energy sources [1]. As the world's largest producer and exporter, Indonesia operates more than 14 million hectares of oil palm plantations, mainly in Sumatra and Kalimantan, making the sector a major contributor to foreign exchange earnings, GDP, and employment for millions of smallholder farmers and industry workers. However, the palm oil processing industry also produces significant waste due to inadequate management and suboptimal utilization, which continues to threaten the environment and public health [2]. One of the abundant solid wastes is oil palm shells, which have not been optimally utilized to date. In fact, oil palm shells contain a high lignocellulose content, consisting of 29.4% lignin, 26.6% cellulose, and 27.7% hemicellulose [3]. The lignin content in this waste can make it potentially suitable for making biochar.

Biochar offers broad potential as a catalyst material due to its long-term stability, high surface area and pore volume, and diverse

surface functional groups. Its applications include esterification/transesterification, tar removal, biodiesel production, biomass hydrolysis, and electrochemical reactions [4]. Recent studies also show that carbon-rich materials from agricultural waste, such as hydrochar produced from rice husks through hydrothermal carbonization, have similar porous structures and functional groups for catalytic and adsorption applications [5]. Similarly, biochar from pine waste activated with HCl has been successfully used for efficient dye removal, demonstrating the importance of activation in enhancing surface reactivity [6], while carbon materials derived from biomass are generally increasingly used for heavy metal remediation [7]. These characteristics make biochar a sustainable and more environmentally friendly alternative to carbon catalysts based on non-renewable sources [8].

Biochar catalysts are one solution to address the negative impacts of biomass waste. The effectiveness of biochar-based materials is further supported by the successful extraction and utilization of silica from palm oil boiler ash and natural zeolite using the coprecipitation method, thereby providing new avenues for

creating multifunctional catalysts from palm oil industry byproducts [9]. Research on environmentally friendly and efficient catalysts is becoming increasingly important due to the growing need for sustainable energy. One strategic application of biochar-based catalysts is in the upgrading process of bio-oil from biomass pyrolysis. The application of biochar-based catalysts from oil palm bunch waste has been reported in hydrodeoxygenation (HDO) reactions has been reported to be effective for guaiacol conversion. The catalytic process predominantly yielded phenol and cresol as the main products, indicating the ability of biochar to facilitate HDO reactions efficiently [10].

Biomass utilization is not limited to the application of biochar as a catalyst; the liquid product of pyrolysis, bio-oil, can also play an important role as feedstock in fuel conversion efforts. However, on the other hand, bio-oil produced from the pyrolysis of oil palm shells still contains high levels of oxygen and water, has high viscosity and corrosive properties, so its quality does not meet liquid fuel standards. The hydrodeoxygenation reaction has shown promise in improving the poor physicochemical properties of oil [11]. The effectiveness of this approach has been demonstrated in various previous studies. The hydrodeoxygenation process has been shown to enhance energy recovery, lower the oxygen content and acidity of bio-oil, and minimize carbon loss during upgrading [12]. In addition, the upgrading of pyrolysis oil through hydro-pyrolysis and HDO has been reported to produce higher-quality oil suitable for fuel or diesel precursor applications, while simultaneously reducing coke formation on the catalyst surface [13]. Further improvements in heavy oil quality and its compatibility with gasoline and diesel have also been achieved through HDO reactions conducted in continuous-flow reactor systems [14].

Therefore, this research offers a novelty by utilizing biochar from oil palm shells as a bimetallic catalyst support for the HDO reaction of oil palm shell bio-oil. The main objective is to improve the quality of the pyrolysis bio-oil by reducing oxygen levels and enhancing its physicochemical properties, thus making it closer to liquid fuel standards and potentially applicable as a renewable energy source. Furthermore, the use of biochar-based catalysts and bio-oil feedstock, both of which are products of pyrolysis from oil palm shell waste, strengthens its promising potential as an environmentally friendly biomass waste management solution.

Experimental

Materials

The materials used include oil palm shell waste obtained from PKS PTPN IV Sawit Langkat (North Sumatra, Indonesia). Ammonium molybdate tetrahydrate ($(\text{NH}_4)_6\text{Mo}_7\text{O}_{24}\cdot 4\text{H}_2\text{O}$), nickel (II) nitrate hexahydrate ($\text{Ni}(\text{NO}_3)_2\cdot 6\text{H}_2\text{O}$), KOH, HCl, and cobalt (II) nitrate hexahydrate ($\text{Co}(\text{NO}_3)_2\cdot 6\text{H}_2\text{O}$) were purchased from Merck. Distilled water and double-distilled water were purchased from Brataco, while N_2 gas and H_2 gas were sourced from PT. Tri Gases Medan, Indonesia.

Preparation of oil palm shell waste

Oil palm shell waste samples were taken from palm oil processing plants, then cleaned with running water and dried in the sun to remove any remaining moisture and ensure the samples were dry. Once dry, the samples were cut into small pieces into fine fibers and then ground into a fine powder [15].

Oil palm shell pyrolysis

Approximately 200 g of dry sample was placed in a pyrolysis apparatus at 500 °C for 2 h. This pyrolysis process produces biochar and bio-oil, collected in a container, along with gas as a byproduct [15].

Biochar activation

The pyrolyzed biochar was refluxed with a 2M KOH solution for 3 h at 60 °C. The biochar was then filtered using filter paper and washed with distilled water until the pH was neutral. The biochar was then dried in an oven at 110 °C for 2 h. The dried biochar was washed with 1M HCl solution, and then neutralized and dried in an oven at 110 °C to produce activated biochar (A-Biochar) [16].

Preparation of catalysts

A total of 0.92 g of $(\text{NH}_4)_6\text{Mo}_7\text{O}_{24}\cdot 4\text{H}_2\text{O}$ was dissolved in 500 mL of deionized water, and then 100 g of biochar was added. Subsequently, the resultant mixture was subjected to reflux for a duration of 5 h at a temperature of 80 °C, after which it was dried at 110 °C, resulting in the formation of the Mo/A-Biochar catalyst. In the next step, 0.57 g of cobalt nitrate ($\text{Co}(\text{NO}_3)_2\cdot 6\text{H}_2\text{O}$), previously dissolved in deionized water, was introduced to the Mo/A-Biochar catalyst. The composite mixture underwent reflux for an additional 5 h at 80 °C, followed by drying at 110 °C, and subsequently underwent an oxidation-reduction process at 500 °C for a duration of 2 h, thereby yielding the CoMo/A-Biochar catalyst [17].

Conversely, the NiMo/A-Biochar catalyst was synthesized through the dissolution of 0.92 g of ammonium heptamolybdate tetrahydrate ($(\text{NH}_4)_6\text{Mo}_7\text{O}_{24}\cdot 4\text{H}_2\text{O}$) in 500 mL of deionized water, followed by the addition of 100 g of biochar. The resultant mixture was subjected to

reflux for a period of 5 h at 80 °C and subsequently dried at 110 °C. An amount of 1.627 g of nickel nitrate ($\text{Ni}(\text{NO}_3)_2\cdot 6\text{H}_2\text{O}$), previously dissolved in deionized water, was then added to the mixture. The resultant composite underwent reflux for an additional 5 h at 80 °C, was dried at 110 °C, thereby yielding the NiMo/A-Biochar catalyst.

Characterization of catalysts

The structural characteristics of the catalyst were examined using X-ray diffraction techniques (XRD D8 Advance (Bruker), employing Bragg-Brentano Diffraction). The surface morphology of the catalyst was analyzed using a Scanning Electron Microscope (SEM SU35000), which was equipped with an Energy-Dispersive X-Ray series (EDS Hitachi). Moreover, nitrogen adsorption-desorption evaluations were conducted using a JWGB V-Sorb 2800P. The test data were used to calculate the specific surface area using the Brunauer-Emmett-Teller (BET) method, while the pore volume and pore size were analyzed from the desorption bands using the Barret-Joyner-Halenda (BJH) method.

HDO process

The bio-oil from pyrolysis that will be hydrodeoxygenated is first pre-treated by esterification. This esterification phase is executed by combining the bio-oil with ethanol in a 1:1 (w/w) ratio within a flask, followed by the incorporation of sulfuric acid as a catalyst, constituting 1% (v/v) of the total sample weight. The esterified bio-oil is subsequently hydrodeoxygenated utilizing A-Biochar, CoMo/A-Biochar, and NiMo/A-Biochar catalysts. This HDO process is conducted in a fixed-bed reactor with hydrogen gas introduced for 2 h and is performed at various temperatures (250, 300, and 325 °C), as displayed in [Figure 1](#).

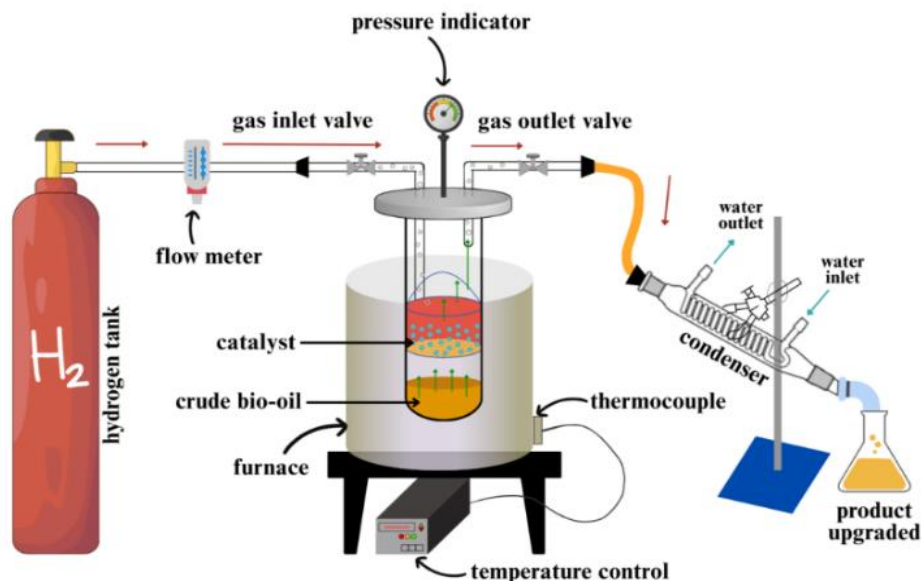


Figure 1. Schematic of fixed-bed reactor for the bio-oil conversion process

Bio-oil characterization

Determination of physicochemical properties before and after the HDO process, including density analysis using a pycnometer, viscosity using an Ostwald viscometer, and acid number using a titration method. The analysis of the compound composition within the bio-oil was executed using Gas Chromatography Mass Spectrometry (GC-MS, Agilent 5977B Mass Selective Detector in conjunction with an Agilent 76938A Autosampler).

Upgrading process optimization

An optimization process is conducted to achieve the best reaction conditions that can produce the desired fuel proportion. In this study, the impact of temperature and catalyst concentration will be analyzed. The impact of temperature will be studied at variations (275, 300, and 325 °C), while the effect of catalyst use will be observed at various catalyst ratios of 1%, 3%, 5%, and 0% (without catalyst).

Results and Discussion

Catalyst characterization

Observations concerning the impact of the modification of Co-Mo and Ni-Mo metal combinations on the biochar carrier were conducted through a comparative analysis of the characteristic peaks present in the XRD diffractograms of each catalyst, as illustrated in [Figure 2](#). The biochar diffractograms indicate that this material has an amorphous structure ([Figure 2a](#)). The characteristic diffraction peak confirming the presence of biochar appears at $2\theta = 22^\circ$. The amorphous structure of biochar provides advantages in catalytic applications because it presents more active surfaces and heterogeneous active sites [4,18].

After chemical activation and modification with metal carriers, there are significant changes as shown in [Figure 2b](#). The peak intensity around $2\theta = 22^\circ$ increases, and there is an additional broad peak around the angle $2\theta = 42.9^\circ$. Post modification via bimetallic metal impregnation, as represented in [Figure 2b](#), the diffractogram

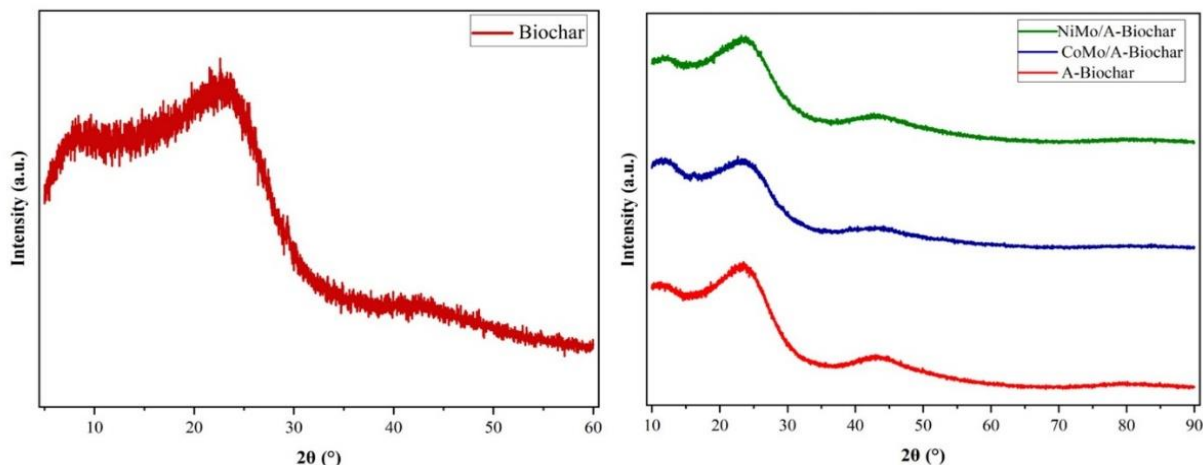


Figure 2. XRD diffractogram of (a) Biochar; (b) A-Biochar (red), CoMo/A-Biochar (blue), and NiMo/A-Biochar (green)

pattern reveals that the principal peaks associated with amorphous carbon continue to dominate at the same 2θ position. However, there is a slight reduction in intensity, which may be attributed to the deposition of metal onto the carbon surface. The incorporation of metals into the catalyst support was observed to reduce the intensity of several major diffraction peaks, while the overall diffractogram profile remained unchanged. This phenomenon indicates that metal impregnation does not damage the structural integrity of the support and suggests that the metals are uniformly distributed within the pore surfaces of the carrier [19]. The surface area, pore volume, and average pore diameter represent crucial characteristics of biochar as a catalyst carrier. Table 1 shows that there are significant changes after activation and bimetallic metal loading on biochar. In its unmodified state, biochar possesses a surface area of $10.597 \text{ m}^2/\text{g}$, a pore volume of 0.030

cm^3/g , and an average pore size of 6.550 nm , which are still low and insufficient to support catalytic activity because the pore structure is still closed or not optimally developed. After activation, the surface area of biochar increases significantly ($218.964 \text{ m}^2/\text{g}$). This indicates that the biochar activation process is exceptionally effective in enhancing and expanding the pore structure, thereby augmenting the number of available active sites. After metal modification into the biochar structure, the catalyst exhibits a reduction in specific surface area and pore volume. This decrease may be caused by penetration and partial blockage of pores by metal particles on the support surface. Although a decrease in surface area was observed following metal impregnation, the remaining surface area, combined with a suitable pore size distribution, remains sufficient to promote the formation of aromatic compounds during catalytic reactions [20]. Furthermore, the

Table 1. Surface area, pore volume, and average pore diameter of the catalysts

Catalysts	Surface area BET (m^2/g)	Pore volume (cm^3/g)	Average pore diameter (nm)
Biochar	10.60	0.030	6.55
A-Biochar	218.96	0.042	4.00
CoMo/A-Biochar	203.06	0.018	4.75
NiMo/A-Biochar	197.11	0.048	5.41

catalysts retained their mesoporous structure after metal impregnation, both NiMo/A-Biochar (5.414 nm) and CoMo/A-Biochar (4.754 nm).

Consequently, the NiMo/A-Biochar and CoMo/A-Biochar catalysts remain viable for utilization in the bio-oil HDO process, as their textural characteristics continue to support catalytic performance, notwithstanding a marginal decline in active biochar. SEM-EDX analysis further revealed the element distribution and surface morphology of the catalyst, shown in Figure 3 and summarized in Table 2. From Figure 3a-b, the raw biochar displayed a relatively smooth surface with minimal pores and uneven distribution, consistent with its low surface area before activation. After activation with KOH (Figure 3(d,e)), the morphology changed to a rougher and more porous one, with open and irregular pores that increased the accessibility of the catalytic sites, as the surface area obtained in Table 1. In CoMo/A-Biochar (Figure 3(g,h)), metal particles were shown to be homogeneously distributed on the surface, while EDX detected Co (approximately 0.8 wt%) and Mo (0.3 wt%) elements with clear spectral peaks, indicating successful impregnation without significant agglomeration that could reduce the catalyst efficiency. Similarly, NiMo/A-Biochar (Figure 3(j,k)) exhibited a similar distribution of Ni (0.4 wt%) and Mo (0.2 wt%), with a smoother surface morphology due to metal deposition, which favored stability during the HDO reaction. These results align with

studies using SEM-EDX to verify the dispersion of bimetallic metals in biochar, where homogeneous distribution improves catalyst stability and reduces deactivation by coke in the bio-oil HDO process [21]. In addition, the EDX spectrum (Figure 3c, 3f, 3i, 3l) showed a decrease in oxygen elements after impregnation on the bimetallic catalyst, indicating a reduction in surface functional groups that facilitate a more efficient HDO reaction, consistent with the findings on biochar catalysts for bio-oil upgrading [22]. This characterization confirmed that bimetallic modification not only maintains the structural integrity of biochar but also improves its catalytic properties, including coke resistance, for bio-oil upgrading applications from biomass waste [23].

Bio-oil composition

GC-MS analysis was conducted on bio-oil derived from oil palm shells subjected to pyrolysis at 550 °C. The area percentages presented in the GC-MS data are presumed to serve as indicators of the concentration levels of each compound component present within the sample. A GC-MS chromatogram depicting crude bio-oil extracted from oil palm shells is illustrated in Figure 4, with the resulting data on the compound components in the bio-oil systematically arranged in Table 3.

Figure 4 indicates that the compounds within the bio-oil are predominantly characterized by phenols, methoxyphenols, and carboxylic acids.

Table 2. Catalyst composition from EDX analysis

Components (Mass%)	Biochar	A-Biochar	CoMo/A-Biochar	NiMo/A-Biochar
C	89.3	85.5	85.9	85.0
O	10.7	14.5	13.1	14.4
Mo	-	-	0.3	0.2
Co	-	-	0.8	-
Ni	-	-	-	0.4

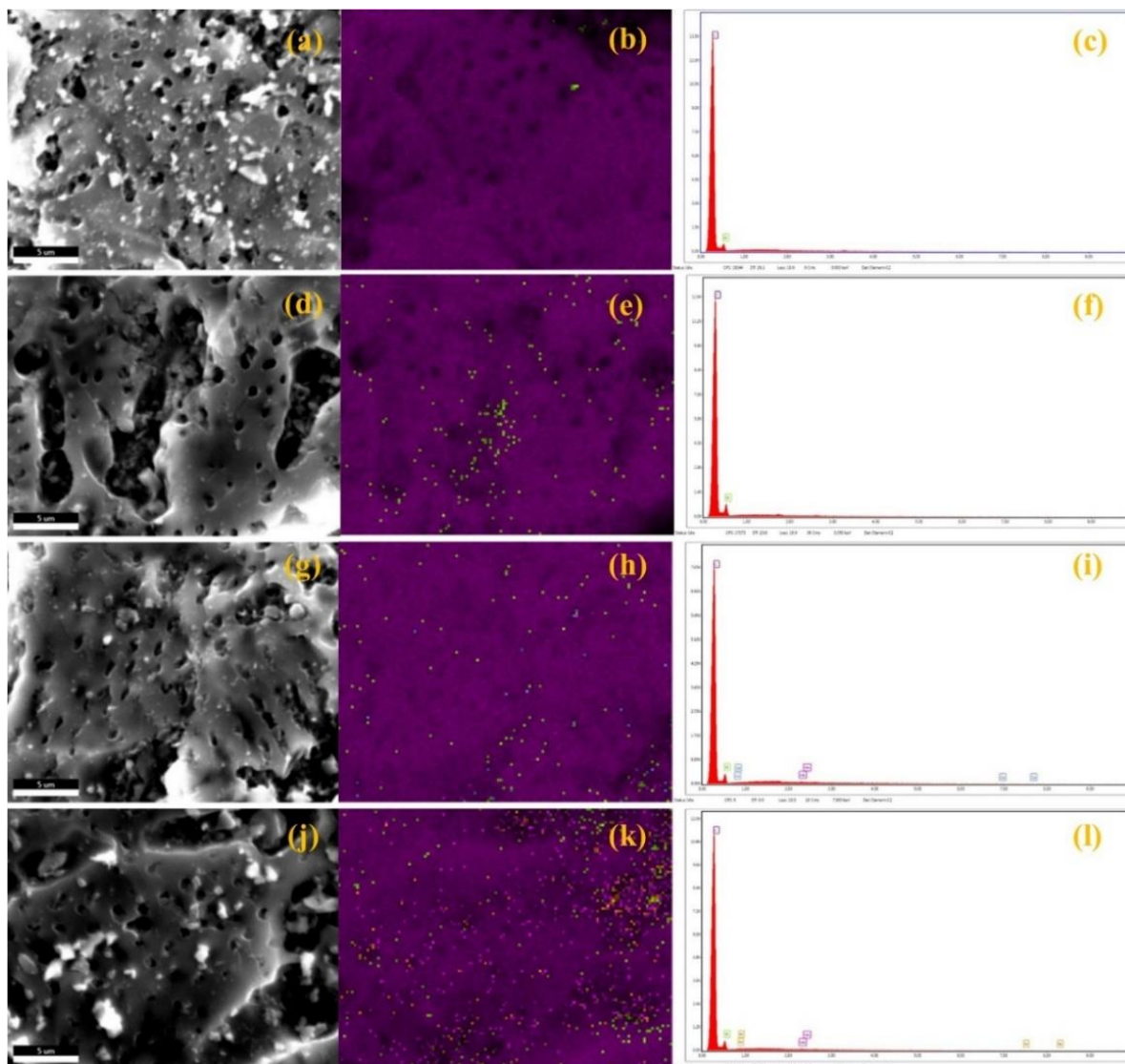


Figure 3. Surface morphology, element mapping, and EDX spectrum of catalyst (a-c) Biochar; (d-f) A-Biochar; (g-i) CoMo/A-Biochar; (j-l) NiMo/A-Biochar. The distribution of elements shows different colors for carbon with purple color, oxygen with green color, nickel with orange color, molybdate with pink color, and cobalt with blue color

Table 3. Composition of raw bio-oil compound from oil palm shells

Compound	RT (min)	Area (%)
2-Cyclopenten-1-one, 2-Methyl-cyclohexanone	6.49	0.3
2,5-Hexanedione	6.629	0.34
Phenol	6.982	0.17
Acetic acid	7.36	29.31
Phenol, 2-Methoxy-catechol	8.469	1.51
Guaicol	8.973	5.29
	10.586	6.89
	10.927	2.98

Benzene, 1-ethyl-4-[(trimethylsilyl) oxyl-	11.078	0.94
Phenol, 2,6-dimethoxy-	12.792	5.51
4-Trimethylsilyloxy-3-methoxybenzyl alcohol	13.334	1.78
2-Anthracenamine	13.724	0.34
3,5-Dimethoxy-4-hydroxytoluene	13.989	2.16
Isoeugenol	14.859	0.86
2-Propanone, 1-(4-hydroxy-3-methoxyphenyl)-	15.048	0.79
Dodecanoic acid	15.388	0.8
anthracene, 1,2-dihydro-10-methyl-	16.711	0.13
Syringylacetone	17.757	0.14
<i>n</i> -Hexadecanoic acid	19.723	0.23

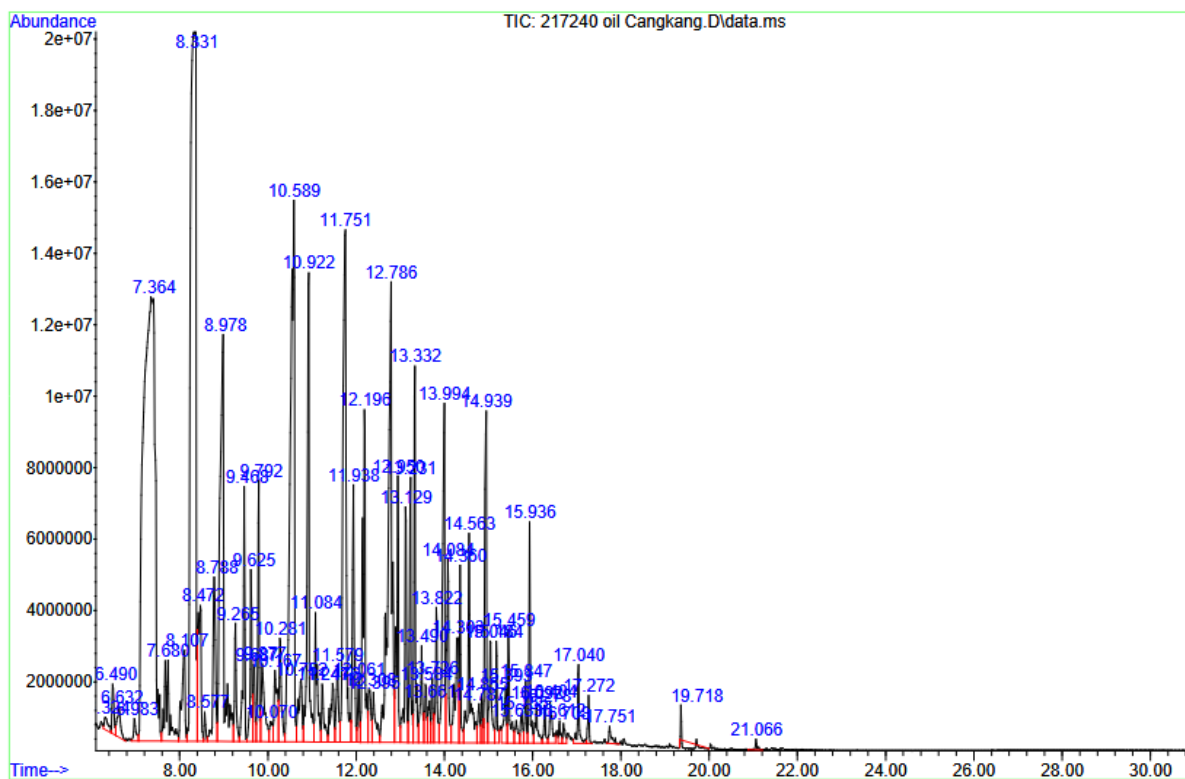


Figure 4. GC-MS chromatogram of raw bio-oil

The compounds identified via pyrolysis are consistent with the lignocellulosic constituents intrinsic to the oil palm shell samples, thereby implying that lignin compounds constitute the majority proportion in comparison to hemicellulose and cellulose. The phenolic compounds represent the most significant percentage, quantified at 29.31%. In the lignin molecular structure, the oxygen bonds

connecting the phenyl-propane units and side branches can easily break when exposed to heat. This dissociation results in the formation of active free radicals characterized by a benzene ring structure, which possess the capability to engage in reactions with other molecules or free radicals, thereby leading to the synthesis of macromolecules that exhibit a more thermodynamically stable configuration,

ultimately culminating in the formation of charcoal.

Hydrodeoxygenation performance

The physicochemical characteristics of bio-oil derivatives were subjected to a comprehensive analysis, encompassing water content, viscosity, density, and acid number. These physicochemical characteristics are systematically presented in Table 4.

Table 4. Physicochemical properties of raw bio-oil

Properties	Raw bio-oil
Water content (%)	66.39
Density (g/cm ³)	1.103
Viscosity (cSt)	6.72
Acid number (mg KOH/g oil)	188.66

According to Table 4, it is apparent that the predominant physicochemical attributes of bio-oil indicate a remarkably high water content, measured at 66.39%. This observation implies that the generation of the H₂O compound is significantly pronounced throughout the decomposition process. A relatively high water content has been reported in bio-oil produced from oil palm biomass pyrolysis, with maximum values reaching up to 76.36%. The elevated oxygen content in bio-oil is closely associated with the high water fraction and the abundance of oxygenated compounds formed during thermal decomposition [24]. The physicochemical characteristics of bio-oil are consistent with those reported for bio-oil derived from various lignocellulosic wastes, where oxygenated compounds dominate the composition and contribute to a high oxygen content [25]. Meanwhile, the presence of oxygenated compounds with a high molecular weight will increase the viscosity and density of

the bio-oil [26]. Reported bio-oil densities range from approximately 1.005 to 1.040 g/cm³, with viscosities reaching up to 23.70 cP (22.79 cSt), indicating that density plays a critical role in combustion behavior by influencing the atomization process [27]. Density is an important parameter in combustion because it can influence the atomization process.

Product distribution

Comparison of HDO products catalyzed by A-Biochar, CoMo/A-Biochar, and NiMo/A-Biochar is shown in Figure 5. The HDO process was carried out at temperature variations of 275 °C, 300 °C, 325 °C on each catalyst. From the distribution graph of HDO products presented in Figure 5, it is discerned that the HDO process catalyzed by A-Biochar, CoMo/A-Biochar, and NiMo/A-Biochar demonstrates a temperature-dependent effect on the liquid phase products generated, with optimal yields at 300 °C, yielding 85.19% (A-Biochar), 80.04% (CoMo/A-Biochar), and 77.78% (NiMo/A-Biochar).

It is established that the yield of liquid phase products obtained at 300 °C correlates with the characteristics of these catalysts, including pore volume, pore diameter, and the metal development ratio, which exhibit minimal variation. The empirical data derived from temperature fluctuations reveal a notable enhancement in the yield of liquid phase products at a temperature of 300 °C; however, an elevation to 350 °C precipitates a stark reduction in the quantities of products produced, specifically a decline of 84.89% for A-Biochar, 68.28% for CoMo/A-Biochar, and 75.08% for NiMo/A-Biochar. This phenomenon exhibits an inverse relationship with the gas output, whereby each of the catalysts—A-Biochar, CoMo/A-Biochar, and NiMo/A-Biochar—

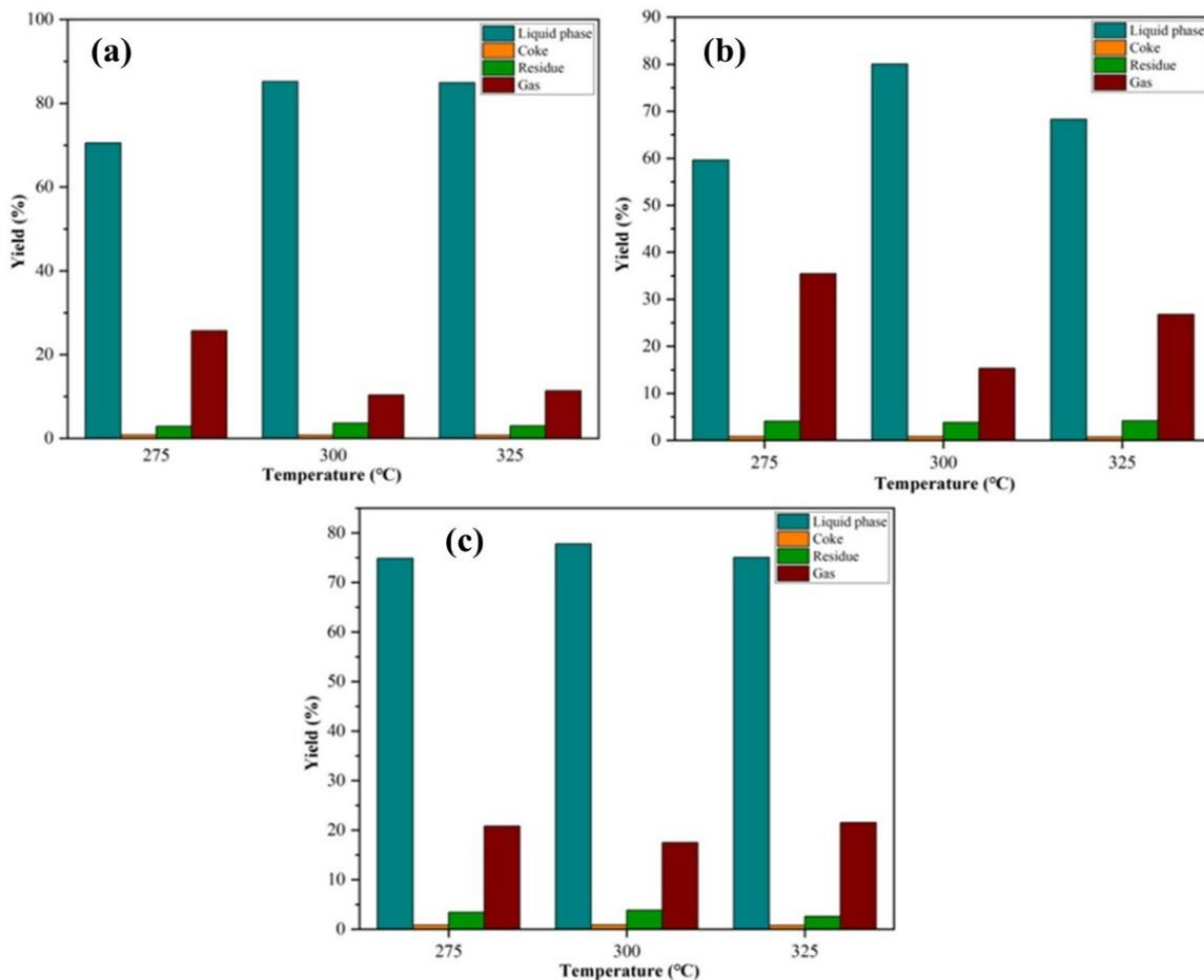


Figure 5. Distribution of upgraded bio-oil products catalyzed by (a) A-biochar; (b) CoMo/A-biochar; and (c) NiMo/A-biochar

displays a decrease at 300 °C (10.38%, 15.32%, and 17.49%, respectively) followed by an increase at 350 °C (11.57%, 26.79%, and 21.53%, respectively). This elevated gas concentration implies that heightened temperatures facilitate the progression of gasification or hydrocracking reactions from bio-oil, thereby transforming organic constituents into gaseous products [28]. The major gaseous products formed during the hydrodeoxygenation process of bio-oil derived from oil palm shells consist primarily of CO, CO₂, CH₄, and other light hydrocarbon gases [29]. In the context of bimetallic catalysts, an increased generation of coke may be discerned as a result

of the swift occupation of Lewis acid sites by oxygenated compounds, while Brønsted acid sites on zeolites promote the transfer of protons to these compounds, ultimately culminating in the formation of carbocation precursors that contribute to coke accumulation on the catalyst interface [30]. The resultant residue appears as a solid, which is likely a consequence of the polymerization and condensation processes of bio-oil throughout the HDO procedure.

Physicochemical properties of upgraded products

The HDO process on bio-oil from oil palm shell pyrolysis has succeeded in significantly improving its physicochemical properties, as

shown in Table 5. The principal properties scrutinized encompass acid value, density, and viscosity. The bio-oil originating from the preliminary pyrolysis exhibited suboptimal physicochemical properties, indicative of corrosiveness, instability, and challenges in its application as a fuel due to its elevated oxygen content [13]. After undergoing the hydrodeoxygenation process in the absence of a catalyst, the acid value of the bio-oil decreased to 57.96 mg KOH/g oil, accompanied by a density of 0.915 g/cm³ and a viscosity of 1.43 cSt. These changes indicate an initial reduction in oxygenated compound content and are consistent with previous observations regarding improvements in bio-oil quality achieved through hydrodeoxygenation reactions [12].

The employment of active biochar catalysts at concentrations of 1%, 3%, and 5% within the HDO reaction progressively enhanced the overall performance. At a concentration of 3% active biochar, the acid number experienced a substantial reduction to 17.92 mg KOH/g oil, accompanied by a density measurement of 0.885 g/cm³ and a viscosity of 1.33 cSt, thereby signifying the efficacy of biochar in the elimination of carboxylic acids and the

augmentation of bio-oil stability. These results are consistent with previous studies reporting the effectiveness of biochar derived from oil palm empty fruit bunches for the hydrodeoxygenation of guaiacol [10]. The bimetallic catalysts CoMo/A-Biochar and NiMo/A-Biochar exhibited markedly superior outcomes.

Specifically, CoMo/A-Biochar at a 1% concentration yielded an acid number of 26.35 mg KOH/g oil, a density of 0.924 g/cm³, and a viscosity of 1.42 cSt, while the 5% CoMo/A-Biochar concentration resulted in values that diminished to 22.89 mg KOH/g oil, a density of 0.879 g/cm³, and a viscosity of 1.47 cSt. The NiMo/A-Biochar catalyst at a concentration of 3% attained the most reduced acid number of 16.47 mg KOH/g oil, a density of 0.703 g/cm³, and a viscosity of 1.29 cSt, which approaches the diesel fuel standard (density approximately 0.85 g/cm³, viscosity roughly 2–4 cSt), indicating a noteworthy reduction in oxygenated compounds and an enhancement in fluidity, in agreement with previous reports on the application of Ni-Mo catalysts for bio-oil hydrodeoxygenation [14].

Table 5. Comparison of the physicochemical properties of raw bio-oil and HDO products

Sample	Acid number (mg KOH/g Oil)	Density (g/cm ³)	Viscosity (cSt)
Raw bio-oil	188.66	1.103	6.72
Without catalyst	57.96	0.915	1.43
1% A-Biochar	34.01	0.937	1.36
3% A-Biochar	17.92	0.885	1.33
5% A-Biochar	19.63	0.895	1.42
1% CoMo/A-Biochar	26.35	0.924	1.42
3% CoMo/A-Biochar	26.68	0.880	1.38
5% CoMo/A-Biochar	22.89	0.879	1.47
1% NiMo/A-Biochar	31.17	0.928	1.39
3% NiMo/A-Biochar	16.47	0.703	1.29
5% NiMo/A-Biochar	21.67	0.878	1.31

Comparative evaluation of the catalysts in the bio-oil HDO reaction demonstrates that NiMo/A-Biochar exhibits superior acidity reduction at higher concentrations, whereas CoMo/A-Biochar provides relatively stable performance across varying catalyst loadings. The observed decrease in density and viscosity is consistent with earlier findings indicating that bimetallic catalysts can effectively improve the physicochemical properties of bio-oil through oxygen removal during HDO reactions, with oxygen reduction reaching up to 29.31% for phenolic compounds [14]. Furthermore, biochar-based catalysts have been reported to enhance hydrocarbon yields in upgraded bio-oil while maintaining environmental sustainability [10]. In conclusion, the results of this study confirm the potential of upgraded bio-oil as a sustainable biofuel. Among the evaluated catalysts, NiMo/A-Biochar demonstrates the most promising performance at concentrations of 3–5%. Nevertheless, further characterization,

including higher heating value (HHV) analysis, is required to comprehensively assess the energy potential of the upgraded bio-oil.

Catalyst selectivity

To evaluate the effectiveness of the HDO process in improving bio-oil quality, GC-MS analysis was performed on the liquid product resulting from the HDO reaction using various catalysts. This analysis aims to identify changes in the distribution of compound groups, specifically a decrease in oxygenated compounds and an increase in hydrocarbons. The findings of this analysis are illustrated in Figure 5, which delineates the area percentage (% area) of the predominant compound classifications within raw bio-oil and subsequent to HDO utilizing activated biochar, CoMo/A-Biochar, and NiMo/A-Biochar catalysts at different proportions of 1%, 3%, and 5%. Based on Figure 6, raw bio-oil is dominated by oxygenated

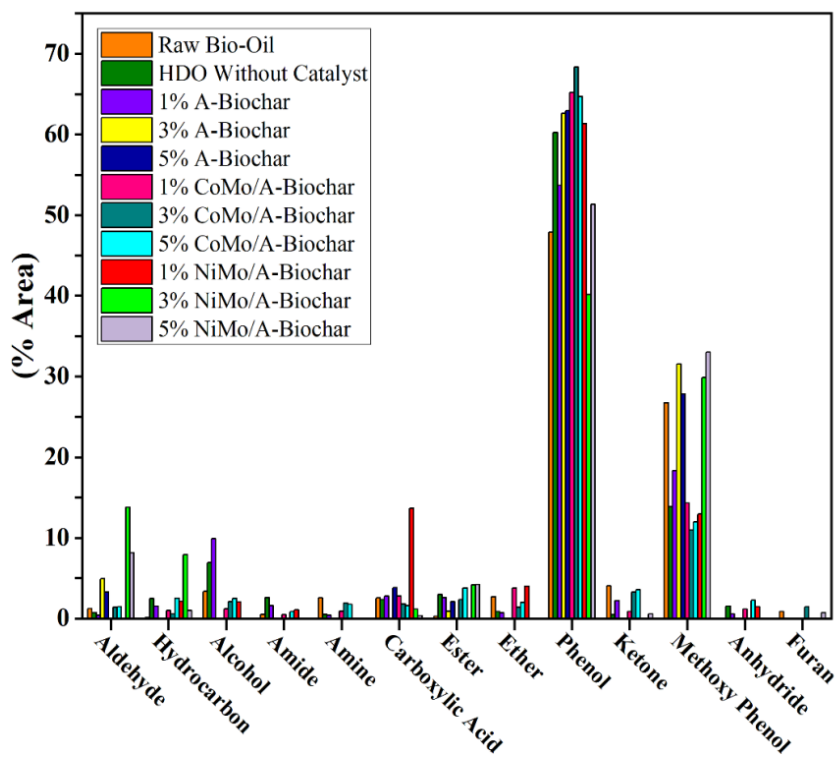


Figure 6. Comparison of the selectivity of raw bio-oil and HDO products

compounds, with phenol reaching 47.92% and methoxyphenol 26.74%, while hydrocarbons are very low (0.13%). The significant presence of oxygenated compounds aligns with the compositional profile of bio-oil derived from the pyrolysis of oil palm shells, which is typically abundant in lignin derivatives such as phenol and guaiacol, resulting in elevated viscosity and diminished stability [31]. Subsequent to the HDO process conducted without a catalyst, there was an augmentation in phenol to 60.24% and a reduction in methoxyphenol to 13.9%, with hydrocarbons experiencing a slight increase to 2.48%, signifying that thermal hydrogenation in isolation is capable of cleaving certain oxygen bonds via the demethoxylation pathway, albeit in a suboptimal manner, and tends to yield phenol as an intermediate product. The use of activated biochar catalyst at ratios of 1%, 3%, and 5% showed more significant improvements in deoxygenation selectivity. At the 1% A-Biochar concentration, the yield of phenol escalated to 53.66%, while methoxyphenol attained 18.35%, with hydrocarbons recorded at a mere 1.55%.

Conversely, at the 3% and 5% ratios, the presence of hydrocarbons was undetected (0%), whereas phenol concentrations reached 62.63% and 62.95%, respectively, alongside methoxyphenol levels of 31.51% and 27.84%. This pattern suggests that activated biochar exhibits greater selectivity for the transformation of methoxyphenol to phenol through the demethoxylation process, albeit demonstrating diminished efficacy in subsequent conversion to hydrocarbons due to the scarcity of hydrogenation sites. Additional functional groups, including carboxylic acids (decreasing from 2.54% in the raw material to 0% in the 3% biochar catalyst, yet increasing to 3.81% in the 5% A-Biochar), ketones (completely lost), and alcohols (also completely lost), similarly exhibited reductions, signifying

the elimination of carboxyl and carbonyl moieties that augment the acidity of bio-oil [32]. The bimetallic catalysts CoMo/A-Biochar and NiMo/A-Biochar exhibited superior performance, particularly at concentrations of 3% and 5%. For the CoMo/A-Biochar configuration, at a 1% ratio, hydrocarbons constituted 0.98%, with phenol at 65.2% and methoxyphenol at 14.31%; at the 3% ratio, hydrocarbons were reduced to 0.55%, while phenol peaked at 68.34% (the highest in this group) and methoxyphenol declined to 10.95% (the lowest within this series); at a ratio of 5%, hydrocarbons ascended to 2.53%, with phenol at 64.7% and methoxyphenol at 11.96%. The synergistic interaction between cobalt, serving as the hydrogenation site, and molybdenum, acting as the deoxygenation facilitator, enabled the preferential conversion of oxygenated compounds to phenol as the predominant intermediate, with minimal selectivity towards hydrocarbons (capped at 2.53%), yet proving effective in diminishing methoxyphenol concentrations to below 12%. In a similar vein, NiMo/A-Biochar demonstrated heightened selectivity for hydrocarbons: at a 1% ratio, hydrocarbons accounted for 2.12%, alongside 61.33% phenol and 12.97% methoxyphenol; at the 3% concentration, hydrocarbons peaked at 7.91% (the highest overall) with phenol declining to 40.16% and methoxyphenol to 29.86%; at the 5% ratio, hydrocarbons decreased to 1%, with phenol at 51.35% and methoxyphenol at 33.02%. This reflects an elevated selectivity towards the comprehensive HDO pathway (for instance, the transformation of guaiacol into cyclohexane via hydrogenolysis and hydrogenation), wherein an optimal Ni/(Ni+Mo) ratio of approximately 3% yields a selectivity of up to 7.91% for hydrocarbons, consequently curtailing the formation of intermediates such as ethers (which were completely lost at 3% and 5%) or amides (also

completely lost at 3%). At a ratio of 1%, performance is lower due to limited metal sites, while a ratio of 5% causes agglomeration that reduces pore accessibility, resulting in lower hydrocarbons. Minor functional groups, including aldehydes (13.79% at 3% NiMo/A-Biochar, but diminishing to 8.17% at 5%), alcohols (completely lost at 3% and 5%), amides (lost at 3%), and furans (lost at 3%), are nearly eliminated or significantly reduced post-HDO with the bimetallic catalyst, indicating a complete conversion to more stable end products [33].

Overall, GC-MS analysis confirmed that the biochar-based bimetallic catalyst was effective in upgrading bio-oil, with a 3% NiMo/A-Biochar ratio being the optimal condition to maximize hydrocarbons (7.91%) and minimize total oxygenates (such as methoxyphenols <30% and phenols ~40%). In comparison, CoMo/A-Biochar was more selective for phenols (up to 68.34%). These results align with the HDO study of bio-oil from palm oil waste, in which oxygen reduction with a bimetallic catalyst increased the calorific value and stability as a biofuel [34]. These improvements not only enhance the potential of bio-oil as a sustainable fuel but also reduce the environmental impact of oil palm shell waste.

Conclusion

This study demonstrated the effectiveness of biochar-based bifunctional catalysts (CoMo/A-Biochar and NiMo/A-Biochar) in the HDO of bio-oil derived from oil palm shell pyrolysis. KOH activation enhanced surface area, while bimetallic modification improved catalytic activity despite minor pore blockage. The optimal reaction at 300 °C yielded up to 85.19% liquid product, as well as a drastic reduction in oxygenate content based on GC-MS analysis. NiMo/A-Biochar achieved the highest hydrocarbon formation (7.91%), whereas

CoMo/A-Biochar exhibited the highest selectivity for phenol (68%). The upgraded bio-oil showed markedly improved fuel properties—lower acidity, viscosity, and density—approaching diesel standards. Overall, oil palm shell-derived biochar catalysts present a sustainable pathway for efficient bio-oil upgrading and renewable fuel production.

Acknowledgments

The authors would like to express their gratitude to the Institute for Research and Community Service (LPPM) at Universitas Negeri Medan for the financial support provided under the Applied Product Research Scheme, with the grant reference No. 0194/UN33/KPT/2025.

Conflict of Interest

No conflicts of interest were declared by the authors in this study.

ORCID

Junifa Layla Sihombing

<https://orcid.org/0000-0001-8977-3701>

Ahmad Nasir Pulungan

<https://orcid.org/0000-0001-9024-6546>

References

- [1] Purnomo, H., Okarda, B., Dermawan, A., Ilham, Q.P., Pacheco, P., Nurfatriani, F., Suhendang, E. [Reconciling oil palm economic development and environmental conservation in indonesia: A value chain dynamic approach](#). *Forest Policy and Economics*, **2020**, 111, 102089.
- [2] Mukhlis, M., Utomo, S., Wijaya, M. [Towards an environmentally friendly palm oil industry: A critical review of waste reduction policies by indonesian government](#). *International Journal of Sustainable Development & Planning*, **2025**, 20(7).
- [3] Wiraya, W.A., Rifaldi, K., Muljani, S., Siswati, N.D., Karaman, N. [Peningkatan kualitas bio-oil hasil pirolisis cangkang kelapa sawit berstandar pelumas organik](#). *Jurnal Fisika Unand*, **2025**, 14(3), 249-254.

- [4] Shan, R., Han, J., Gu, J., Yuan, H., Luo, B., Chen, Y. A review of recent developments in catalytic applications of biochar-based materials. *Resources, Conservation and Recycling*, **2020**, 162, 105036.
- [5] Appazov, N.O., Kanzhar, S., Alimkhan, B., Bekkhozhayev, M., Serikbayev, M., Niyazova, D., Yespanova, I., Toibazarova, A., Tolegenkyzy, M., Lyubchuk, S. Synthesis of hydrochar by hydrothermal carbonization of rice husk. *Advanced Journal of Chemistry, Section A*, **2026**, 9(2), 265-274.
- [6] Z, F., Frida, E., Susilawati, S., Ginting, E.M., Humaidi, S., Tarigan, J. Comparison of the effectiveness of the coprecipitation method for SiO₂ extraction from natural paha zeolite and palm oil boiler ash. *Advanced Journal of Chemistry, Section A*, **2025**, 8, 1578.
- [7] Aljeboree, A.M., Hadi, E.S., Alalqa, I.S., Hussein, T.K., Altimari, U.S., Alkaim, A.F. Efficient removal of cationic and anionic dyes using hcl-activated biochar from pine waste: Adsorption behavior and thermodynamic insights. *Advanced Journal of Chemistry, Section A*, **2025**, 8(7), 1233-1246.
- [8] Musheer, N., Yusuf, M., Choudhary, A., Shahid, M. Recent advances in heavy metal remediation using biomass-derived carbon materials. *Advanced Journal of Chemistry, Section B: Natural Products and Medical Chemistry*, **2024**, 6(3), 281-342.
- [9] Garg, U., Azim, Y. Biochar-based catalysts for the production of chemical and energy. *Biochar: A Sustainable Approach*, **2024**, 169-189.
- [10] Adilina, I.B., Widjaya, R.R., Hidayati, L.N., Supriadi, E., Safaat, M., Oemry, F., Restiawaty, E., Bindar, Y., Parker, S.F. Understanding the surface characteristics of biochar and its catalytic activity for the hydrodeoxygenation of guaiacol. *Catalysts*, **2021**, 11(12), 1434.
- [11] Gea, S., Hutapea, Y.A., Piliang, A.F.R., Pulungan, A.N., Rahayu, R., Layla, J., Tikoalu, A.D., Wijaya, K., Saputri, W.D. A comprehensive review of experimental parameters in bio-oil upgrading from pyrolysis of biomass to biofuel through catalytic hydrodeoxygenation. *BioEnergy Research*, **2023**, 16(1), 325-347.
- [12] Eschenbacher, A., Saraeian, A., Shanks, B.H., Jensen, P.A., Li, C., Duus, J.Ø., Hansen, A.B., Mentzel, U.V., Henriksen, U.B., Ahrenfeldt, J. Enhancing bio-oil quality and energy recovery by atmospheric hydrodeoxygenation of wheat straw pyrolysis vapors using pt and mo-based catalysts. *Sustainable Energy & Fuels*, **2020**, 4(4), 1991-2008.
- [13] Shafaghat, H., Linderberg, M., Janosik, T., Hedberg, M., Wiinikka, H., Sandstrom, L., Johansson, A.C. Enhanced biofuel production via catalytic hydro-pyrolysis and hydro-coprocessing. *Energy & Fuels*, **2021**, 36(1), 450-462.
- [14] Oh, S., Lee, J.H., Choi, J.W. Hydrodeoxygenation of crude bio-oil with various metal catalysts in a continuous-flow reactor and evaluation of emulsion properties of upgraded bio-oil with petroleum fuel. *Renewable Energy*, **2020**, 160, 1160-1167.
- [15] Pulungan, A.N., Kembaren, A., Sihombing, J., Ginting, C., Nurhamidah, A., Hasibuan, R. The stabilization of bio-oil as an alternative energy source through hydrodeoxygenation using co and co-mo supported on active natural zeolite. *Journal of Physics: Conference Series*, **2022**, 2193(1), 012084.
- [16] Lü, F., Lu, X., Li, S., Zhang, H., Shao, L., He, P. Dozens-fold improvement of biochar redox properties by koh activation. *Chemical Engineering Journal*, **2022**, 429, 132203.
- [17] Allwar, A., Maulina, R., Julianto, T.S., Widyaningtyas, A.A. Hydrocracking of crude palm oil over bimetallic oxide nio-cdo/biochar catalyst. *Bulletin of Chemical Reaction Engineering & Catalysis*, **2022**, 17(2), 476-485.
- [18] Astuti, F., Sari, N., Maghfirohtuzzoimah, V.L., Asih, R., Baqiya, M.A., Darminto, D. Study of the formation of amorphous carbon and rgo-like phases from palmyra sugar by variation of calcination temperature. *Jurnal Fisika Dan Aplikasinya*, **2020**, 16(2), 91.
- [19] Sihombing, J.L., Gea, S., Wirjosentono, B., Agusnar, H., Pulungan, A.N., Herlinawati, H., Yusuf, M., Hutapea, Y.A. Characteristic and catalytic performance of Co and Co-Mo metal impregnated in Sarulla natural zeolite catalyst for hydrocracking of MEFA rubber seed oil into biogasoline fraction. *Catalysts*, **2020**, 10, 121.
- [20] Zheng, Y., Wang, J., Li, D., Liu, C., Lu, Y., Lin, X., Zheng, Z. Activity and selectivity of Ni-Cu bimetallic zeolites catalysts on biomass conversion for bio-aromatic and bio-phenols. *Journal of the Energy Institute*, **2021**, 97, 58-72.
- [21] Wang, S., Li, H., Wu, M. Advances in metal/biochar catalysts for biomass hydro-upgrading: A review. *Journal of Cleaner Production*, **2021**, 303, 126825.
- [22] Ji, X., Tian, X., Zhou, M., Chen, C., Jiang, J. Ni-mofs and lignin modified biochar: An environmentally-friendly and efficient catalyst for catalytic transfer hydrodeoxygenation of lignin derivatives. *Industrial Crops and Products*, **2025**, 223, 120162.
- [23] Ma, X., Zhou, B., Budai, A., Jeng, A., Hao, X., Wei, D., Zhang, Y., Rasse, D. Study of biochar properties by scanning electron microscope-energy dispersive x-ray spectroscopy (sem-edx). *Communications in Soil Science and Plant Analysis*, **2016**, 47(5), 593-601.
- [24] Sakulkit, P., Palamanit, A., Dejchanchaiwong, R., Reubroycharoen, P. Characteristics of pyrolysis products from pyrolysis and co-pyrolysis of rubber

wood and oil palm trunk biomass for biofuel and value-added applications. *Journal of Environmental Chemical Engineering*, **2020**, 8(6), 104561.

[25] Abatyough, M.T., Ajibola, V.O., Agbaji, E.B., Yashim, Z.I. Properties of upgraded bio-oil from pyrolysis of waste corn cobs. *Journal of Sustainability and Environmental Management*, **2022**, 1(2), 120-128.

[26] Fekhar, B., Zsinka, V., Miskolczi, N. Thermo-catalytic co-pyrolysis of waste plastic and paper in batch and tubular reactors for in-situ product improvement. *Journal of Environmental Management*, **2020**, 269, 110741.

[27] Qureshi, K.M., Lup, A.N.K., Khan, S., Abnisa, F., Daud, W.M.A.W. Optimization of palm shell pyrolysis parameters in helical screw fluidized bed reactor: Effect of particle size, pyrolysis time and vapor residence time. *Cleaner Engineering and Technology*, **2021**, 4, 100174.

[28] Ahmadi, S., Reyhanitash, E., Yuan, Z., Rohani, S., Xu, C.C. Upgrading of fast pyrolysis oil via catalytic hydrodeoxygenation: Effects of type of solvents. *Renewable Energy*, **2017**, 114, 376-382.

[29] Ly, H.V., Kim, J., Hwang, H.T., Choi, J.H., Woo, H.C., Kim, S.S. Catalytic hydrodeoxygenation of fast pyrolysis bio-oil from *saccharina japonica* alga for bio-oil upgrading. *Catalysts*, **2019**, 9(12), 1043.

[30] Gea, S., Irvan, Wijaya, K., Nadia, A., Pulungan, A.N., Sihombing, J.L., Rahayu Bio-oil hydrodeoxygenation over zeolite-based catalyst: The effect of zeolite activation and nickel loading on product characteristics. *International Journal of Energy and Environmental Engineering*, **2022**, 13(2), 541-553.

[31] Mansur, D., Rahayu, E.P., Fitriady, M.A., Simanungkalit, S.P. Hydrodeoxygenation of palm kernel shells derived bio-oil using supported ru and pd catalysts. *ChemistrySelect*, **2022**, 7(10), e202102436.

[32] Kuchonthara, P., Reubroycharoen, P., Hinchiranan, N. Quality improvement of oil palm shell-derived pyrolysis oil via catalytic deoxygenation over nimos/ γ -Al₂O₃. *Fuel*, **2015**, 143, 512-518.

[33] Mishra, R.K., Kumar, D.J.P., Sankannavar, R., Binnal, P., Mohanty, K. Hydro-deoxygenation of pyrolytic oil derived from pyrolysis of lignocellulosic biomass: A review. *Fuel*, **2024**, 360, 130473.

[34] Muangsuwan, C., Kriprasertkul, W., Ratchahat, S., Liu, C.G., Posoknistakul, P., Laosiripojana, N., Sakdaronnarong, C. Upgrading of light bio-oil from solvothermal liquefaction of an oil palm empty fruit bunch in glycerol by catalytic hydrodeoxygenation using nimo/Al₂O₃ or como/Al₂O₃ catalysts. *ACS Omega*, **2021**, 6(4), 2999-3016.

HOW TO CITE THIS MANUSCRIPT

J.L. Sihombing, A.N. Pulungan, H. Herlinawati, T. Ramadhani, S.N.B. Sinaga, S. Salaisa, D. Fahreza, M.F.A. Saragih. Bifunctional Biochar-Supported Catalysts for Efficient Hydrodeoxygenation of Pyrolytic Oil Derived from Oil Palm Shells. *Asian Journal of Green Chemistry*, 10 (4) 2026, 548-564.

DOI: <https://doi.org/10.48309/ajgc.2026.552702.1846>

URL: https://www.ajgreenchem.com/article_238871.html